Macromolecules

ARTICLE

pubs.acs.org/Macromolecules

Water-Soluble Conjugated Polyelectrolytes with Branched Polyionic Side Chains

Seoung Ho Lee, Sevnur Kömürlü, Xiaoyong Zhao, Hui Jiang, Gustavo Moriena, Valeria D. Kleiman, and Kirk S. Schanze*

Department of Chemistry, University of Florida, Gainesville, Florida 32611-7200, United States

Supporting Information

ABSTRACT: A new series of conjugated polyelectrolytes (CPE) consisting of an arylene−ethynylene backbone featuring phenyl (Ph), 2,1,3-benzothiadiazole (BTD), or 4,7-bis(2′-thienyl)-2,1,3-benzothiadiazole (TBT) units have been synthesized and characterized. On each polymer repeat unit the CPEs contain two branched ionic side groups each featuring a "triad" of carboxylate ($R\text{-}CO_2^-Na^+$) or ammonium ($R\text{-}NH_3^+Cl^-$) units, giving the polymers six ionic charges per repeat. The photophysical properties of the series of CPEs were investigated in CH_3OH and H_2O solution by absorption, steady-state fluorescence, and fluorescence lifetime spectroscopy. The different arylene units in the backbone lead to the variation of the HOMO−LUMO gap across the series. The branched, polyionic side chains suppress aggregation of the polymer chains, even in aqueous solution, leading to higher fluorescence quantum yields relative to similar CPEs with linear side chains. UV−vis absorption spectra show that CPEs with anionic branched side chains ($R\text{-}^bCO_2^-Na$) aggregate at low pH, while retaining the photophysical properties of their organic-soluble precursors at high pH. CPEs having branched cationic side chains ($R\text{-}^bNH_3^+Cl^-$) exhibit the opposite response to pH change.

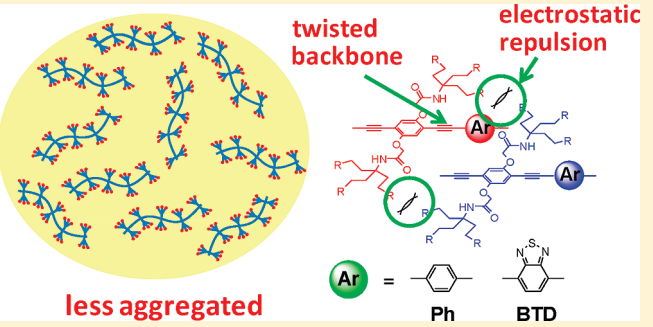

INTRODUCTION

Over the past several years, conjugated polyelectrolytes (CPEs) have attracted considerable attention as versatile materials in optoelectronic devices and biochemical detection systems.[1−4] Their high fluorescence quantum yields, extreme sensitivity to fluorescence quenchers (amplified quenching), and electrostatic interactions with oppositely charged species in solution provide a unique opportunity for sensor applications.[5−10] The quenching response of CPEs to oppositely charged quenchers is amplified due to intra- and interchain exciton migration and because ionic quenchers can form strong association complexes with CPEs and aggregates.[2,5,11−13] A variety of fluorescent sensors based on electron or energy transfer have been developed to take advantage of aggregation between water-soluble CPEs and added analytes.[13−16] For example, Wang and Bazan observed that significant enhancement of fluorescence emission in polymer aggregates is due to shielding effect of the polymer backbone from water contact.[17] This result may encourage development of highly sensitive chemical sensors even in aqueous solution with high salt concentration.

In spite of the potential advantages of CPEs in sensor applications, their properties are sometimes limited by a low fluorescence quantum yield, poor solubility, and unpredictable sensor response induced by their strong propensity to self-assemble into aggregates in aqueous solution.[18−21] There has been some effort devoted to suppress aggregation and increase the fluorescence quantum yield in aqueous media by varying the solvent polarity, pH, and ionic strength.[22−24] Unfortunately, the conditions required to suppress aggregation are often inconsistent with detecting analytes in biological media. Furthermore, the fluorescence quantum yield showed relatively small enhancement.[23]

Aggregation occurs due to the hydrophobic nature of the conjugated polymer backbones or, under certain salt conditions, because of electrostatic interaction between the side chains of the CPEs,[2,24,25] leading to decreased solubility.[2,18] To overcome this drawback in aqueous solution, Swager reported the introduction of a sterically hindered repeat unit into the CPE backbone, inducing less aggregation in a slightly twisted polymer structure.[18]

In the present investigation, we explore the properties of two series of conjugated polyelectrolytes that feature sterically congested, branched polyionic side groups (Scheme 1). This series was designed to explore the ability of bulky, highly charged ionic functional groups on the CPE side chains to reduce the hydrophobic interchain interactions by increasing the electrostatic repulsion between polymer chains. The large number of ionic groups is expected to enhance the solubility of the CPE in aqueous solutions. Furthermore, modulation of the aggregation process by adjusting the pH can afford some control to avoid unexpected sensing behavior.[18−21,26] An additional advantage of

Received: March 14, 2011
Revised: May 13, 2011
Published: June 03, 2011

Scheme 1. Structure of CPEs with Branched Polyanionic or Cationic Side Chains[a]

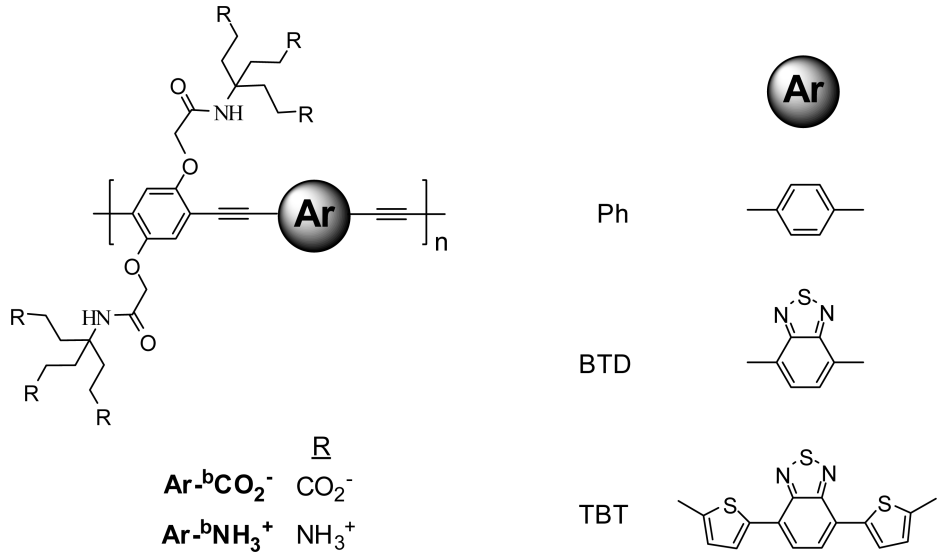

[a] The superscript "b" refers to the branched ionic side groups.

Scheme 2. Polymerization through Precursor Route[a]

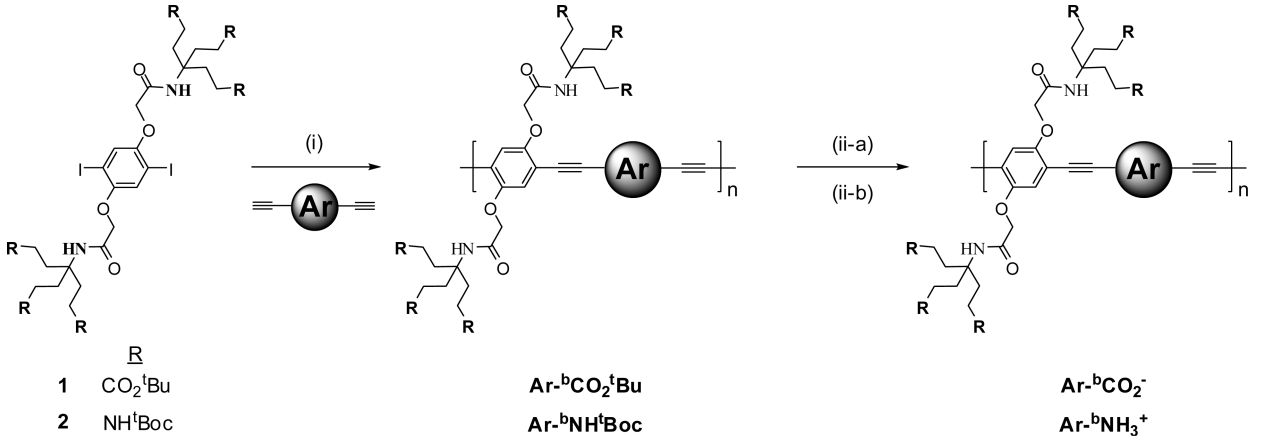

[a] Ar = Ph, BTD, and TBT. (i) $Pd(PPh_3)_4$, CuI, THF/TEA (3/1, v/v), (ii-a) Ph and BTD: TFA/DCM for anionic polymer; 4 N HCl/dioxane for cationic polymer; TBT: $ZnBr_2$, DCM/H_2O, (ii-b) saturated Na_2CO_3 aqueous solution for anionic polymer.

using branched ionic side chains is the creation of a receptor with a three-dimensional structure which can provide a cavity which is able to exhibit specific binding to ions and/or biomolecules.[27] The combination of these structural advantages with optical probes sensitive to perturbation by external stimuli can provide effective fluorescence sensors resulting in more effective polymer-based transducers for sensory application.

RESULTS AND DISCUSSION

Polymer Synthesis and Characterization. Herein we report the synthesis and photophysical characterization of a new family of arylene−ethynylene-based water-soluble CPEs with branched ionic side chains. The aryl groups phenyl (Ph), 2,1,3-benzothiadiazole (BTD), or 4,7-bis(2′-thienyl)-2,1,3-benzothiadiazole (TBT) units are introduced into the CPE backbone to modulate their photophysical properties (Scheme 1). Negatively or positively charged branched, polyionic side chains are added to hinder aggregation of the polymer chains and suppress self-quenching of the excited state of the CPE. Synthetic details for the synthesis of monomers **1** and **2** is provided in the Supporting Information.

Scheme 2 shows the route used for synthesis of all of the "precursor" organic-soluble polymers by Sonogashira coupling of a stoichiometric amount of the monomer with branched side chains (**1** or **2**) and a diacetylene substituted arylene comonomer. The polymerization was carried out in organic solution using organic-soluble ester or amide precursors in order to avoid electrostatic repulsion of the ionic charged functional groups and to facilitate polymer characterization by organic phase gel permeation chromatography (GPC). The number- and weight-average molecular weights (M_n and M_w, respectively) for the polymer samples were estimated by GPC analysis of the organic soluble ester or amide precursors (Table 1).

Hydrolysis of the precursors for anionic and cationic CPEs was accomplished in acidic solution. TBT-$^bCO_2{}^tBu$ decomposed in acidic or basic solution; thus, its hydrolysis was performed under

dx.doi.org/10.1021/ma200574d |*Macromolecules* 2011, 44, 4742–4751

Table 1. GPC Analysis of Precursor Polymers

	precursor polymers (GPC)[a]		
acronym	M_n (kDa)	M_w (kDa)	PDI
Ph-^{b}CO_2^{t}Bu	33.2	112.0	3.00
BTD-^{b}CO_2^{t}Bu	11.7	16.3	1.40
TBT-^{b}CO_2^{t}Bu	16.8	37.8	2.26
Ph-^{b}NH^{t}Boc	24.1	105.6	4.40
BTD-^{b}NH^{t}Boc	12.3	44.7	3.60

[a] Estimated by GPC (THF), polystyrene standards.

mild conditions using zinc bromide and water (in the acronyms the "b" superscript refers to the branched side groups).[28] The resulting polymer solutions were treated with saturated Na_2CO_3 (no further treatment for cationic CPEs) and then purified by dialysis using 12 kDa molecular weight cutoff (MWCO) dialysis membranes. The water-soluble branched anionic and cationic CPEs were obtained as solids in 90−100% yield, based on the organic soluble precursor.

Figure S1 shows representative ^{1}H NMR spectra of the monomer **1**, the precursor polymer Ph-^{b}CO_2^{t}Bu, and the water-soluble polymer Ph-^{b}CO_2^-. Comparison of the spectra of monomer **1** and Ph-^{b}CO_2^{t}Bu reveals that there is only one new resonance peak in the spectrum of the latter at δ = 7.58 ppm, assigned to the aromatic protons of 1,4-phenylene on the polymer backbone. The *tert*-butyl protons appear as a strong singlet at δ = 1.42 ppm in the spectra of monomer **1** and Ph-^{b}CO_2^{t}Bu. After hydrolysis, the ^{1}H NMR spectrum of Ph-^{b}CO_2^- was measured in DMSO-d_6/D_2O (1/1, v/v) mixture. No signals were observed in the 1.4−1.5 ppm range, indicating that the *tert*-butyl groups were cleaved efficiently (>95%). Changes in the infrared (IR) absorption spectra corresponding to the ester carbonyl group also support the removal of the *tert*-butyl ester. Similar patterns were observed for the other deprotected polymers in which more than 95% of the peak arising from the *tert*-butyl groups disappear in the ^{1}H NMR and IR spectra.

The photograph in Figure 1 illustrates the colors of the anionic CPEs under visible and near-UV illumination. Ph-^{b}CO_2^- appears pale yellow by eye, while its fluorescence is bright blue-white; BTD-^{b}CO_2^- appears red in visible light, with a bright red fluorescence; TBT-^{b}CO_2^- is purple, whereas its fluorescence is dark purple. Corresponding photographs of the cationic pair of CPEs, Ar-^{b}NH_3^+ are shown in Figure S2.

Photophysical Properties and the Influence of Solvent. The photophysical properties of the series of CPEs were investigated by steady-state UV−vis absorption and fluorescence spectroscopy. When the HOMO−LUMO energy gap is varied by changing the aryl group from Ph to BTD to TBT, a red-shift is observed in both absorption and emission spectra for the series of anionic CPEs (Figure 2). The effect of the solvent is observed in spectra collected in a "good" solvent (CH_3OH), a "poor" solvent (H_2O), and a mixture (CH_3OH/H_2O (1/1, v/v)). In methanol, Ph-^{b}CO_2^- exhibits an absorption maximum at 403 nm and a fluorescence maximum at 433 nm while its cationic counterpart, Ph-^{b}NH_3^+ (Figure S3), exhibits similar spectra with maxima at 402 nm (absorption) and 432 nm (emission). Complete spectra for the cationic pair of polymers are shown in the Supporting Information, and characteristic wavelengths are listed in Table 2.

In previous work, we have characterized the photophysical properties of CPEs with linear ionic side chains, PPE-CO_2^-, PPE-SO_3^-, and PPE-BTD-SO_3^- (Scheme 3). When the absorption

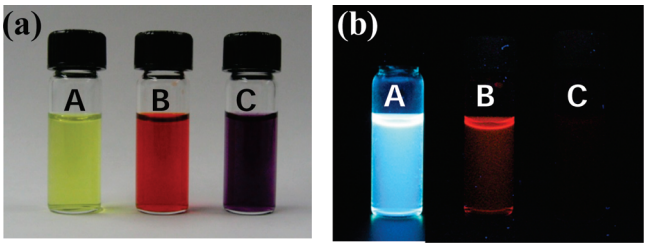

Figure 1. Photographs under (a) visible and (b) near-UV illumination for solutions of (A) Ph-^{b}CO_2^-, (B) BTD-^{b}CO_2^-, and (C) TBT-^{b}CO_2^-; [Ar-^{b}CO_2^-] = 30 μM in H_2O.

spectra of Ph-^{b}CO_2^- and Ph-^{b}NH_3^+ in methanol are compared to those of PPE-CO_2^- and PPE-SO_3^-,[12,25,29,30] a blue-shift of ~15−22 nm is observed for the former pair of CPEs. Given that the degree of polymerization (DP) for Ph-^{b}CO_2^- and Ph-^{b}NH_3^+ is ~20 arylene ethynylene units, the blue-shifts are believed to be a consequence of the branched side chains. It is likely that the high ionic charge and size of the side groups interrupt the coplanarity of the conjugated backbone due to increased steric and electronic repulsion between the side chains.[19] However, the influence of the branched side chain upon the CPEs ground electronic state is not observed in the excited state of the polymers. In particular, the fluorescence emission of Ph-^{b}CO_2^- and Ph-^{b}NH_3^+ in the good solvent methanol is very similar to that of the counterparts shown in Scheme 3.[12,29] This lack of energy difference in the fluorescence emission indicates that in the excited state the polymer backbone is able to undergo planarization, resulting in a singlet exciton with maximized delocalization throughout the phenylene ethylene chain.

We observed a similar influence of the branched side chains when the arylene ethynylene backbone contains the BTD-ethynylene unit. In particular, methanol solutions of BTD-^{b}CO_2^- and BTD-^{b}NH_3^+ exhibit visible absorption maxima at 491 and 493 nm, respectively. When compared to structurally similar CPEs with linear side chains, these polymers exhibit blue-shifts in the absorption of 23 and 21 nm, respectively, while their fluorescence spectra are not shifted with respect to reference polymers with linear ionic side chains.[29] It is evident from comparison of the spectra of the new polymers with those of previously reported systems that the optical properties of this family of arylene ethynylene conjugated polyeletrolytes are determined mainly by the electronic structure of the π-conjugated backbone. The photophysical properties are only weakly modulated by the structure and charge of the ionic side chains.[29]

The effect of the branched side chains on aggregation of the CPEs was investigated by comparing their optical properties in H_2O, CH_3OH, and a H_2O/CH_3OH mixture (poor, good, and intermediate solvents, respectively).[25,29] In previous work, we found that the absorption and fluorescence emission spectra of PPE-SO_3^- in methanol are characterized by a sharp, structured emission with only a small Stokes shift, indicating the presence of the polyelectrolyte in a nonaggregated state. In aqueous solution this CPE is aggregated, and this results in a red-shifted UV−vis absorption spectrum with a pronounced shoulder and a fluorescence spectrum with a broad, red-shifted "excimer-like" structure. Excitation spectra of PPE-CO_2^- show a strong detection wavelength dependence, indicating the presence of aggregates, even in the good solvent methanol.[31] Lacking bulky or highly charged side chains, these polyelectrolytes have a tendency to

dx.doi.org/10.1021/ma200574d |*Macromolecules* 2011, 44, 4742–4751

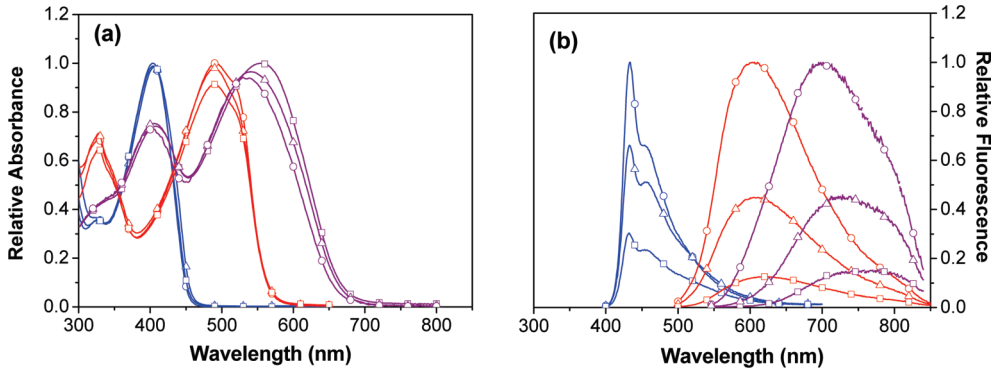

Figure 2. (a) Relative absorption and (b) fluorescence emission spectra of Ph-$^{b}CO_2^-$ (blue), BTD-$^{b}CO_2^-$ (red), and TBT-$^{b}CO_2^-$ (purple) in CH_3OH (○), CH_3OH/H_2O (1/1, v/v) (△), and H_2O (□); [Ar-$^{b}CO_2^-$] = 5 μM.

Table 2. UV−vis Absorption and Emission Properties of CPEs Containing Branched Carboxylate or Ammonium Side Groups

	CH_3OH			H_2O		
acronym	λ_{max}^{abs}/nm	λ_{max}^{em}/nm	Φ_{PL}	λ_{max}^{abs}/nm	λ_{max}^{em}/nm	Φ_{PL}
Ph-$^{b}CO_2^-$	403	433	0.31[a]	404	432	0.12[a]
BTD-$^{b}CO_2^-$	491, 530 (sh)	605	0.04[b]	490, 530 (sh)	623	0.007[b]
TBT-$^{b}CO_2^-$	529	698, 780 (sh)	0.028[b]	536	741, 780 (sh)	0.004[b]
Ph-$^{b}NH_3^+$	402	432	0.45[a]	405	432	0.13[a]
BTD-$^{b}NH_3^+$	493	604	0.04[b]	489, 530 (sh)	620	0.004[b]

[a] Coumarin 102 in EtOH as the standard, Φ_{FL} = 0.95. [b] $Ru(bpy)_3Cl_2$ in H_2O as standard, Φ_{FL} = 0.036.

Scheme 3. Structure of CPEs with Linear Side Chains

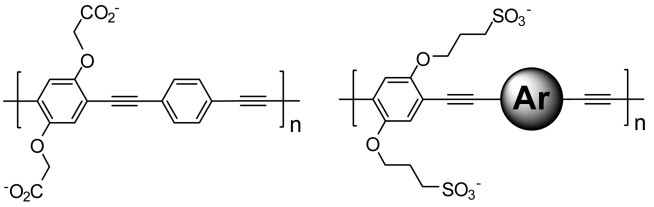

PPE-CO_2^- **PPE-SO_3^-** Ar

Ph

PPE-BTD-SO_3^- BTD

adopt a coplanar structure concomitant with aggregation, and the tendency to aggregate is enhanced in aqueous solution where it is driven by hydrophobic interactions among the aromatic hydrocarbon units comprising the polymer backbone.[32]

Figure 2 (Ph-$^{b}CO_2^-$) and Supporting Information Figure S3 (Ph-$^{b}NH_3^+$) show the response of the absorption and fluorescence of these CPEs to solvent. Notable is that fact that for both polymers there is negligible change in the wavelength maxima or spectral band shape for the absorption and fluorescence spectra as the volume fraction of H_2O in the solvent increases. Indeed, the spectral band shapes resemble those of the corresponding organic-soluble precursor polymers in a good organic solvent where aggregation is minimal (Figure S4). The only noticeable change is a small reduction in the fluorescence quantum yield (Table 2) on going from CH_3OH to H_2O solvent. In addition, the excitation spectrum[33] of Ph-$^{b}CO_2^-$ in CH_3OH (Figure S5) shows no wavelength dependence, suggesting that unlike the CPEs with linear side chains, Ph-$^{b}CO_2^-$ and Ph-$^{b}NH_3^+$ are less likely to aggregate, even in H_2O solution. The presence of the branched polyionic side chains induces a torsional strain within the PPE backbone to minimize electrostatic repulsion, and this torsion impedes the coplanarization of chains and subsequent aggregation.

Incorporation of the benzothiadiazole (BTD) unit into the backbone in BTD-$^{b}CO_2^-$ and BTD-$^{b}NH_3^+$ leads to a slight decrease of the absorption coefficient as the H_2O content increases. We did not observe any wavelength shift in the absorption of BTD-$^{b}CO_2^-$ (even in 100% water), although the excitation spectrum in methanol (Figure S5) exhibits a weak dependence on detection wavelength. The absorption spectrum of BTD-$^{b}NH_3^+$ (Figure S3) undergoes only a small red-shift as water is added to the solution. Simultaneously, a strong decrease in the emission quantum yield and small red shifts (18 and 16 nm, respectively) are observed for both BTD-$^{b}CO_2^-$ and BTD-$^{b}NH_3^+$ as the amount of water in the solvent increases (Figure 2 and Table 2). These effects may suggest that the BTD-containing polymers undergo some aggregation in aqueous solution.

On the basis of our previous work, we expect that strong aggregation will give rise to a much larger red-shift (>30 nm) in both the absorption and emission spectra of the BTD-containing polymers.[34,35] Specifically, in a previous study of PPE-BTD-SO_3^- (Scheme 3) it was found that this polymer exhibits an ~40 nm red-shift in the absorption and fluorescence spectra as the solvent is changed from CH_3OH to H_2O.[29] By contrast, Huang et al.[19] showed that modest red-shifts (<20 nm) in both UV−vis and emission spectra are induced by planarization of the conjugated backbone.

An alternative explanation for the fluorescence red-shift and quenching observed for BTD-$^{b}CO_2^-$ and BTD-$^{b}NH_3^+$ is that

dx.doi.org/10.1021/ma200574d |Macromolecules 2011, 44, 4742–4751

there is an intramolecular charge transfer interaction between the dialkoxyphenylene (donor) and the benzothiadiazole (acceptor) repeat units that is enhanced in the more polar aqueous solution. Donor−acceptor chromophores are known to exhibit fluorescence red-shifts and decreased quantum yield in polar solvents as observed for the BTD-containing CPEs.[36] In summary, we posit that while there may be some aggregation of BTD-$^{b}CO_2^-$ and BTD-$^{b}NH_3^+$ water-rich solution, the majority of solvent induced changes in the fluorescence arise because of the existence of donor−acceptor interactions in these polymers.

The notion that aggregation does not occur to a significant extent for Ph-$^{b}CO_2^-$ and BTD-$^{b}CO_2^-$ (as well as their cationic counterparts) is also supported by their comparatively large fluorescence quantum yields in aqueous solution (Table 2). In particular, the fluorescence quantum yields of Ph-$^{b}CO_2^-$ and BTD-$^{b}CO_2^-$ are significantly larger than the yields of CPEs with the same backbone but with linear ionic side chains.[25,29,30] The enhanced fluorescence yields for Ph-$^{b}CO_2^-$ and BTD-$^{b}CO_2^-$ are observed in both CH_3OH and H_2O; however, the effect is more pronounced in H_2O, supporting the idea that electrostatic repulsion among the polyionic, branched side chains plays an important role in suppressing aggregation.

The CPE with the lowest HOMO−LUMO gap (TBT-$^{b}CO_2^-$) exhibits a different solvent dependence compared to the other CPEs. Specifically, with increasing volume fraction of water the absorption and fluorescence of TBT-$^{b}CO_2^-$ are significantly red-shifted by 29 and 43 nm, respectively (Figure 2). In pure methanol, the fluorescence spectrum exhibits a maximum at 698 nm with a shoulder at ∼780 nm. With increased volume fraction of water, the emission maximum shifts to 741 nm while the relative contribution from the shoulder grows, and it becomes the predominant emission feature in pure water. These spectral changes are combined with a gradual decrease in the fluorescence intensity (quantum yield) with increasing H_2O content. We have previously observed that excitation spectroscopy is more sensitive to aggregation than absorption.[31] Although the presence of unique spectral features arising from aggregates are not observed in the absorption of TBT-$^{b}CO_2^-$, the existence of aggregates is evident from the wavelength dependence of the fluorescence excitation spectra. Specifically, excitation spectra detected at 650 and 800 nm (Figure S5) show two bands shifted by 25 nm, confirming the presence of two distinct absorbing chromophores (two distinct ground state populations) even in methanol solution.

There are two possible contributions to the observed bands in the absorption, emission and excitation spectra of TBT-$^{b}CO_2^-$. First, charge-transfer character in the excited state leads to a red-shift in fluorescence spectra as the H_2O fraction increases. The benzothiadiazole group within the TBT unit is a strong electron acceptor while the flanking thienylene units are electron donors, giving rise to a charge-separated excited state. The excited state is stabilized in the more polar solvent (water) with the effect being more pronounced in TBT-$^{b}CO_2^-$ than in BTD-$^{b}CO_2^-$ and BTD-$^{b}NH_3^+$ because of the stronger donor character of the thienylene units.[37] Second, the presence of the long wavelength shoulder (780 nm) is an indication of aggregate emission induced by hydrophobic interchain interactions. The observed red-shift with increased volume fraction of H_2O in the absorption and the fluorescence excitation spectra also support the presence of aggregates in TBT-$^{b}CO_2^-$.[12] In this polymer there is a greater distance separating the ionic side chains and the carbon atom number:charge ratio is larger; these features reduce electrostatic repulsion between the ionic side chains and increase the hydrophobicity of the polymer. Both effects increase the propensity of the CPE to undergo aggregation in water.

From the spectral changes observed within this series of CPEs (with branched polyionic side chains and Ph, BTD, and TBT groups in the backbone), we conclude that there is a moderate influence of the arylene groups on aggregation. For the small arylene units (Ph and BTD), steric hindrance and electrostatic interaction between the branched side chains effectively suppress aggregation, while hydrophobic interactions are more predominant when the larger TBT group allows for cofacial alignment inducing more polymer aggregation. Importantly, the results suggest that the Ph and BTD polymers do not aggregate to a significant extent in water, and this leads to enhancement in their fluorescence properties.

pH Effects: Aggregation Induced by Variation of pH. In previous studies of water-soluble CPEs, it has been observed that electrostatic repulsion among anionic side chains can be decreased by protonation of weakly acidic groups (or deprotonation of weakly basic groups).[17,38] Consequently, changes in the solution pH yield different degrees of aggregation, and this effect (observed in both anionic and cationic CPEs) is reflected in the efficiency of energy transfer and quenching.[17,24,39]

We investigated the effect of pH on the absorption and fluorescence spectra of the series of anionic and cationic CPEs, Ar-$^{b}CO_2^-$, and Ar-$^{b}NH_3^+$. The pH-dependence experiments were performed in aqueous solution in which the pH was adjusted by addition of HCl and/or NaOH. The goal was to vary the extent of CPE aggregation by controlling the protonation state of the carboxyl (amine) groups. As outlined below, specific changes are seen in the optical spectra as a function of decreased (or increased) pH. In each case the spectral changes were only partially reversible upon readjustment of the pH following the initial decrease (or increase). This partial irreversibility is likely due to precipitation of the polymer from solution when the ionic charge is fully eliminated by protonation (or deprotonation).

Figure 3 shows the absorption and fluorescence emission spectra of Ph-$^{b}CO_2^-$ and Ph-$^{b}NH_3^+$ in aqueous solution as a function of pH. At pH 10.5, the anionic CPE, Ph-$^{b}CO_2^-$, exhibits a single, featureless absorption band with a maximum at 404 nm and fluorescence with a maximum at 435 nm and well-defined vibronic structure. The fluorescence is characteristic of a molecularly dissolved poly(phenylene ethynylene) polymer.[35] As pH decreases, the absorption shifts to lower energy, and a shoulder on the red side of the spectrum (435 nm) grows in, becoming the predominant feature at pH 4.5. An isosbestic point is observed at 410 nm, suggesting a pH-induced transformation between two distinct chromophores. In addition, the fluorescence spectrum changes significantly as pH is decreased. Specifically, the intensity of the 435 nm band decreases, while simultaneously, a very broad, lower energy band appears. At pH 4.5, fluorescence from the nonaggregated CPE is completely quenched, and only the band at 515 nm is detected. These results reveal aggregation of Ph-$^{b}CO_2^-$ at low pH induced by charge neutralization accompanied by conformational change of the PPE backbone. As pH decreases, the ionic side chains become protonated; as such, electrostatic repulsion between the carboxylate groups decreases, reducing the tendency of the phenylene ethynylene backbone to twist out of coplanarity. In addition, water solvation decreases near the neutral side chains, and the more hydrophobic environment leads to the planarization of the conjugated backbone.

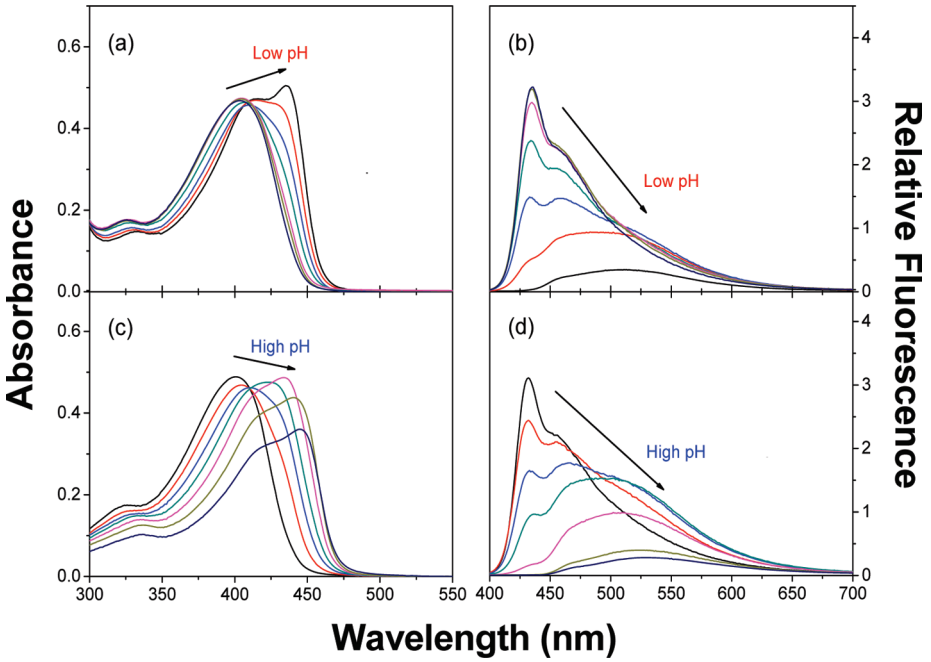

Figure 3. Absorption and fluorescence emission spectra of (a, b) Ph-$^{b}CO_2^-$ and (c, d) Ph-$^{b}NH_3^+$ as a function of pH in aqueous solution; [Ph-$^{b}CO_2^-$ or $^{b}NH_3^+$] = 5 μM. pH varied from 10.5 to 4.5 in (a, b) and from 4.5 to 10.5 in (c, d). In each case the increment is 1.0 pH unit.

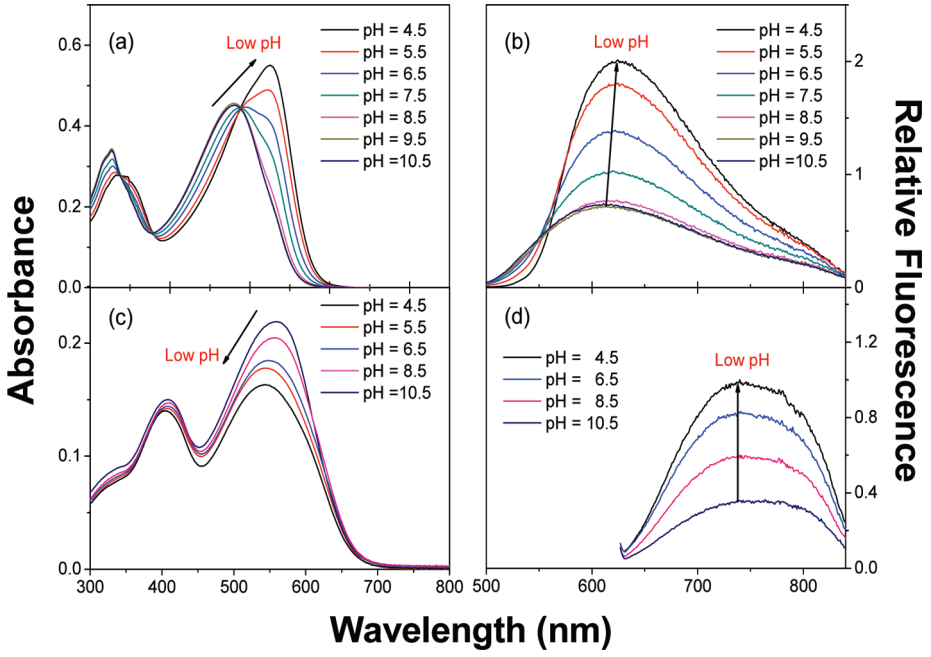

Figure 4. Absorption and fluorescence emission spectra of (a, b) BTD-$^{b}CO_2^-$ and (c, d) TBT-$^{b}CO_2^-$ as a function of pH in aqueous solution; [Ar-$^{b}CO_2^-$] = 5 μM.

Similar to Ph-$^{b}CO_2^-$, the cationic Ph-$^{b}NH_3^+$ showed aggregation that is pH-dependent; however, in this case increased pH leads to aggregation as expected for a weakly basic, cationic CPE. Figures 3c,d show the absorption and emission spectra of Ph-$^{b}NH_3^+$ at different pH levels. At low pH (4.5) the absorption and fluorescence spectra retain the characteristics of molecularly dissolved chains, while at high pH (10.5) they exhibit red-shifted bands, decrease of the high energy fluorescence, and low quantum yield emission. From pH 4.5 to 8.5, an isosbestic point is observed in the absorption spectra due to ionic and neutral polymers. At higher pH, the absorption decreases significantly likely due to precipitation of fully deprotonated polymer chains.

The pH-dependent absorption and emission changes of BTD-$^{b}CO_2^-$ and BTD-$^{b}NH_3^+$ are shown in Figures 4a,b and Figure S6, respectively. The absorption spectra show similar changes than those found for Ph-$^{b}CO_2^-$ and Ph-$^{b}NH_3^+$: a shoulder on the red side of the spectrum that grows as pH decreases (pH increases for Ph-$^{b}NH_3^+$) and an isosbestic point

dx.doi.org/10.1021/ma200574d |*Macromolecules* 2011, 44, 4742–4751

Table 3. Fluorescence Lifetimes (τ_i, ns) and Relative Amplitudes (RA, %) for Ar-$^{b}CO_2^-$ in CH_3OH and Basic (pH 9.0) and Acidic (pH 4.5) Water[a]

	CH_3OH			H_2O, pH 9.0			H_2O, pH 4.5		
acronym	RA (%)			RA (%)			RA (%)		
Ph-$^{b}CO_2^-$	τ_i (ns)[b]	430 nm	500 nm	τ_i (ns)	430 nm	500 nm	τ_i (ns)	430 nm	500 nm
	τ_1 = 0.21	32	17	τ_1 = 0.08	55	36	τ_1 = 0.25	94	54
	τ_2 = 0.52	64	70	τ_2 = 0.23	42	52	τ_2 = 1.30	5	24
	τ_3 = 1.76	3	11	τ_3 = 1.29	2	6	τ_3 = 4.57	<1	22
	τ_4 = 4.67	<1	<2	τ_4 = 4.19	<1	<6			
	χ^2	0.977	1.068	χ^2	1.016	1.112	χ^2	1.173	1.042
BTD-$^{b}CO_2^-$	τ_i (ns)	600 nm	650 nm	τ_i (ns)	600 nm	650 nm	τ_i (ns)	600 nm	650 nm
	τ_1 = 0.27	34	28	τ_1 = 0.17	92	93	τ_1 = 0.25	58	59
	τ_2 = 0.92	48	47	τ_2 = 1.11	6	4	τ_2 = 0.92	41	39
	τ_3 = 2.38	18	25	τ_3 = 5.10	<2	<3	τ_3 = 5.20	1	<2
	χ^2	1.105	1.143	χ^2	1.112	1.273	χ^2	1.243	1.153

[a] Data were analyzed by the global fitting algorithm. [b] Typical limits of error in τ_i are less than ±3%.

revealing two states with distinct absorption. In contrast, the fluorescence spectra show unexpected behavior compared to CPEs having phenylene repeats (Figure 4b and Figure S6b). In particular, the fluorescence emission of BTD-$^{b}CO_2^-$ narrows and increases in intensity as pH decreases. At pH = 4.5, greater than 3-fold intensity enhancement is observed (at 640 nm) compared to pH 10.5. Wang and Bazan found a similar result for a CPE that contains benzothiazole as one of the repeat units.[17] They proposed that lower pH enhances the emission from the benzothiadiazole groups due to shielding from water in the aggregated state of the polymer. Interestingly, we found a similar result in the fluorescence emission changes of BTD-$^{b}NH_3^+$ in basic solution (pH = 10.5, Figure S6b). In both cases, BTD-$^{b}CO_2^-$ and BTD-$^{b}NH_3^+$, the absorption shows the signature of aggregation, and under the conditions where aggregation is observed the emission is enhanced. Clearly, the enhanced emission intensity is due to less water contact with the conjugated backbone induced by the formation of polymer aggregates. The nonradiative decay pathways in polar solvents that decrease the emission yield of the charge transfer excited state are minimized when the side chains become protonated and therefore less solvated. Although no direct evidence is in hand, it is possible that there are specific hydrogen-bond interactions taking place between the BTD unit and water molecules that enhance the nonradiative decay rate of the fluorescent singlet state. Similar effects are known for small molecule heterocyclic chromophores.[40]

When the BTD group is replaced by the TBT unit (TBT-$^{b}CO_2^-$), a small blue-shift (16 nm) is observed in the absorption spectra (Figure 4c) with decreasing pH, but an isosbestic point is not observed. The emission shown in Figure 4d arises completely from the aggregated form (compare with Figure 2b), but the intensity is enhanced as pH decreases from 10.5 to 4.5.

Fluorescence Decay Dynamics. The presence of aggregates in the CPE systems provides for dynamic interaction among exciton states in nonaggregated chains and excitons localized on aggregate (trap) sites. We have previously showed that in the case of CPEs with linear side chains (e.g., PPE-SO_3^- and PPE-CO_2^-) energy transfer to and quenching by aggregate (trap) states occurs leading to changes in the fluorescence decay dynamics.[31] In the present investigation, in order to gain insight into the photophysical properties of the CPEs with branched side chains, we measured their fluorescence decay dynamics as a function of solvent polarity and pH by using time-correlated single photon counting (TCSPC).

Table 3 shows the fitting parameters for solutions of two representative anionic CPEs, Ph-$^{b}CO_2^-$ and BTD-$^{b}CO_2^-$, in pure methanol and in water at pH 9.0 and 4.5. All the CPEs exhibit multiexponential decay dynamics with components ranging from 100 ps to 5 ns. Here we provide a phenomenological description of the fitted decay kinetics, including lifetimes (τ_i) and relative amplitude contributions (RA%) to the overall decays. The nonexponential decay behavior arises due to the existence of an inhomogeneous distribution of chromophores within the complex system consisting of molecularly dissolved chains and aggregate states. In addition, conformational disorder within individual CPE chains yields a distribution of chromophores corresponding to conjugated segments with different lengths. Methanol solutions of anionic (Table 3) and cationic (Table S1) CPEs gave very similar results. For the aqueous solutions, anionic and cationic CPEs feature complementary results in acid or basic solutions. Here we focus on the anionic systems to understand the effects induced by the different protonation and solvation conditions.

Analysis of the emission decay of Ph-$^{b}CO_2^-$ in methanol yields four decay components, with the fastest two (0.21 and 0.52 ns) contributing to 96% ($\lambda_{detection}$ = 430 nm) and 87% ($\lambda_{detection}$ = 500 nm) of the overall amplitude. Under basic conditions (pH 9.0) in water, the fit of the emission decay of Ph-$^{b}CO_2^-$ also features four decay constants. Similar results are obtained when monitoring the emission at 430 and 500 nm with the two fast components (0.080 and 0.23 ns) contributing a combined 97% (at 430 nm) and 88% (at 500 nm) of the overall amplitudes. Of these two components, the slowest one has a larger amplitude contribution in methanol. Table 2 shows that the quantum yield in methanol is slightly larger than in water, a difference consistent with an overall slower fluorescence decay rate. This means that the lower fluorescence quantum yield in water for this CPE is due to enhanced nonradiative decay in the more polar solvent environment.

At pH 4.5 in water the lifetime distribution for Ph-$^{b}CO_2^-$ is quite different. The sub-nanosecond decay constant (0.25 ns) becomes the sole contributor to 94% of the amplitude when

detection is at the short wavelength region of the spectrum (430 nm). When detected at 500 nm, the amplitude of the fast component decreases to 54%, while long-lifetime components (τ = 1.30 and 4.57 ns) contribute significantly to the amplitude (46%).

There are two issues to consider with respect to the fluorescence decay dynamics of Ph-$^{b}CO_2^-$. First, the wavelength dependence of the amplitudes is an indication of multiple emissive units; in this case, aggregated and molecularly dissolved chains present at low pH. Second, at longer wavelengths, the contribution is greater from the slower components. It is expected that the emission decays more slowly at longer wavelength, where the contribution from the aggregate states is larger.[31,41] Similar results of lifetime changes were found in the studies of the aggregation of CPEs having linear side chains, in which the lifetimes were wavelength-dependent and the analysis of ultrafast components provided a model of energy transfer between the different components.[18,31] These observations further support the conclusion that aggregation of Ph-$^{b}CO_2^-$ is minimal in methanol and in aqueous solution at pH 9.0 due to repulsion between the fully ionized branched side chains; however, the degree of aggregation in water increases with decreasing pH, leading to a complex mixture of molecularly dissolved and aggregated chains in weakly acidic solution (pH 4.5).

The fluorescence decay obtained from solutions of BTD-$^{b}CO_2^-$ in pure CH_3OH features comparable contributions from three components. Decays monitored at 600 and 650 nm show similar behavior, with τ = 0.27, 0.92, and 2.38 ns. In basic aqueous solution (pH 9.0), the decay of BTD-$^{b}CO_2^-$ is dominated by a short-lived component (τ = 0.17 ns, >90%). Interestingly, however, at pH 4.5, the emission decays *more slowly*, with ~60% of the amplitude corresponding to τ = 0.25 ns and ~40% to τ = 0.92 ns, with little dependence on the emission wavelength. The short lifetime of the emission in basic aqueous solution (where the polymer is not aggregated) and the increase at low pH where aggregation is expected to be significant are consistent with the notion that the emission from this polymer comes from a singlet state with considerable charge-transfer character. When the polymer is aggregated at low pH, interaction of the chains with the polar aqueous solvent environment is decreased, and the nonradiative decay rate is decreased, leading to an enhanced fluorescence yield and increased lifetime.

Taken together, the emission decay kinetics data reveal that the singlet excited state decay behavior of the CPEs is complex. For the phenylene-based polymer, in a nonaggregated state (methanol and basic water) the decay kinetics are relatively wavelength independent with lifetimes in the 100−300 ps time domain, which is typical for PPE-type conjugated polymers where the singlet decay is dominated by the radiative decay pathway (with high quantum yield). When the polymer is aggregated, the decay kinetics become wavelength dependent. At short wavelength the decay is rapid, presumably due to energy transfer from solvated chains to aggregate trap sites. At longer wavelength the lifetime is longer, reflecting the lower radiative decay rate for the aggregate states. The behavior of BTD-$^{b}CO_2^-$ polymers is even more complex, presumably due to the charge-transfer character of the singlet excited state. The most interesting observation for this system is that the decay kinetics are very rapid when the polymer is not aggregated in water, but they slow significantly when the polymer is aggregated, presumably due to shielding of the conjugated chains from the aqueous environment.

SUMMARY AND CONCLUSIONS

We have successfully prepared and characterized a new series of conjugated polyelectrolytes based on the poly(arylene ethynylene) backbone and featuring branched anionic (R-$^{b}CO_2^-$) or cationic (R-$^{b}NH_3^+$) side chains. These polymers were prepared using a "precursor route"[2] in which organic soluble ester (or carbamate) protected monomers were polymerized in an organic solvent via a Sonogashira coupling reaction. Hydrolysis of the precursor polymers followed by dialysis in aqueous solutions afforded CPEs with branched, polyionic side chains terminated by anionic (carboxylate) or cationic (ammonium) groups. Varying the structure of arylene units in the conjugated backbone induces variation of the HOMO−LUMO gap, producing a series of CPEs with tunable band gap, exhibiting visually different colors in absorption and fluorescence.

Investigation of the photophysical properties of the CPEs leads to the conclusion that the polymers with phenylene and benzothiadiazole repeats are relatively free from aggregation in methanol and aqueous solution (under appropriate pH conditions). The molecularly dissolved CPEs exhibit superior photophysical properties, including enhanced fluorescence quantum efficiency and spectral distribution compared to previously studied CPEs with linear side chains. The improved properties can be used to advantage when the CPEs are applied in sensor schemes, and a recent study highlights this fact.[27] Unfortunately, the polymer with the lowest band gap, TBT-$^{b}CO_2^-$, is aggregated even in the good solvent CH_3OH, and to a greater extent in aqueous solution, presumably due to decreased electrostatic repulsion between side chains because of the relatively large size of the TBT repeat unit. In addition, pronounced charge transfer character of the excited state in this polymer induces a significant red-shift in the emission. Because of the aggregation and relatively weak, red-shifted emission, TBT-$^{b}CO_2^-$ is not a particularly useful CPE for fluorescence sensor applications.

The pH dependence of the absorption and fluorescence spectra for the CPEs demonstrated that the state of aggregation is affected by changing the degree of protonation (or deprotonation) of the weakly acidic (or basic) side groups. In particular, the anionic CPEs are relatively free from aggregation in water at high pH, but the chains become aggregated as the pH of the solution is decreased below 7. The cationic CPEs exhibit a complementary pH-dependent response (aggregation at high pH and molecularly dissolved at low pH).

Taken together, the results presented herein describe an interesting new set of CPEs which may find potential use in sensor or optoelectronic applications.[2−4] The parent polymer of this series, Ph-$^{b}CO_2^-$, is relatively easy to synthesize in good yield, and the polymer is easily stored in the solid state. This CPE exhibits a relatively high emission quantum yield (~12%) in aqueous solution, and the fluorescence spectrum is not affected by the excimer-like emission that dominates the emission of many poly(arylene ethynylene) type CPEs in aqueous solution. Future studies will seek to take advantage of the superior photphysical properties of this novel class of conjugated polyelectrolytes.[27]

EXPERIMENTAL SECTION

Instrumentation and Methods. NMR spectra were recorded using a Varian VXR-300 FT NMR, operating at 300 MHz for ^{1}H NMR

and at 75 MHz for ^{13}C NMR. Gel permeation chromatography (GPC) analyses were carried out on a system comprised of a Rainin Dynamax SD-200 pump, Polymer Laboratories PL gel mixed D columns, and a Beckman Instruments Spectroflow 757 absorbance detector. Molecular weight calibration was effected by using polystyrene standards. UV−vis absorption spectra were recorded on a Varian Cary 50 spectrophotometer. Steady-state fluorescence spectra were obtained with a PTI fluorometer. A 1 cm quartz cuvette was used for all spectral measurements. Fluorescence quantum yields are reported relative to know standards (coumarin 102, $\Phi = 0.95$[42] in EtOH; $Ru(bpy)_3Cl_2$, $\Phi = 0.036$[43,44] in H_2O). Lifetime measurements were carried out using a PicoQuant FluoTime 100 compact fluorescence lifetime spectrometer. The pH of aqueous solution was adjusted with HCl and/or NaOH using a Corning pH meter 320.

Synthesis. General Polymerization Procedure. Monomer **1** or **2** (0.25 mmol) and 0.25 mmol of the other monomers (1,4-diethynylbenzene (Ph), 4,7-diethynyl-2,1,3-benzothiadiazole (BTD), or 4,7-bis-[2′-(5′-ethynyl)thienyl]-2,1,3-benzothiadiazole (TBT)) were dissolved in 16 mL of THF/Et_3N (3/1, v/v). The resulting solution was deoxygenated with argon for 15 min. Then $Pd(PPh_3)_4$ (17.3 mg, 15.0 μmol) and CuI (5.7 mg, 30.0 μmol) were added to the stirred solution under the protection of argon. The reaction mixture was then heated up to 60−65 °C and stirred for 24 h. The viscous solution was then poured into 200 mL of methanol. The precipitate was collected by vacuum filtration and washed with methanol (200 mL). After drying under vacuum, the polymer was stored as a solid. Typical reaction yields for the polymerization are 80−90%.

Hydrolysis of Precursor Polymers. (a) Polymers with Ph or BTD repeats: The organic precursor polymer was dissolved in 20 mL of CH_2Cl_2 and cooled in an ice/water bath. Trifluoroacetic acid (TFA, 20 mL) was added dropwise to the polymer solution. Upon completion of the addition, the reaction mixture was allowed to warm to room temperature and stirred for another 12 h. Excess TFA and solvent were removed *in vacuo*. (b) Polymer with TBT repeat: to a solution of the organic precursor polymer in 20 mL of CH_2Cl_2/DMSO (3/1, v/v), $ZnBr_2$ was added and the solution stirred for 24 h. At this time, 20 mL of water was added, and the mixture was stirred for 1 h. The layers were separated, and the organic solvent was removed *in vacuo*; the residue was treated with saturated aqueous Na_2CO_3 solution (10 mL) and stirred at room temperature for 3 h. The solution was then poured into 200 mL of acetone. In all cases they hydrolyzed polymers were dissolved in water and purified by dialysis using 12 kDa MWCO regenerated cellulose membranes (yield: 90−100%). The water-soluble polymers could be stored either as aqueous solutions or as solid powders.

Ph-^{b}CO$_2$^{t}Bu. ^1H NMR (500 MHz, $CDCl_3$, δ_{ppm}): 7.60 (br, s, 4H), 7.07 (s, 2H), 6.42 (s, 2H), 4.52 (s, 4H), 2.16 (br, m, 12H), 1.98 (br, s, 12H), 1.42 (s, 54 H). ^{13}C NMR (125 MHz, $CDCl_3$, δ_{ppm}): 172.3, 166.8, 132.2, 81.0, 58.0, 46.6, 29.8, 28.1, 8.9. GPC (THF, polystyrene standard): $M_w = 33\,230$, $M_n = 101\,210$, PDI = 3.00. FT-IR (ν_{max}, KBr pellet): 3403, 2978, 2935, 2205, 1731, 1692, 1532, 1512, 1484, 1456, 1410, 1393, 1368, 1312, 1282, 1256, 1214, 1154, 1101, 1051, 954, 891, 848, 758.

Ph-^{b}CO$_2$Na. ^1H NMR (300 MHz, D_2O/DMSO-d_6 (v/v, 1/1), δ_{ppm}): 7.58 (br, 4H), 7.16 (s. 2H). 5.25 (s, 4H). FT-IR (ν_{max}, KBr pellet): 3391, 2937, 2202, 1665, 1564, 1404, 1283, 1208, 1099, 1053, 892, 847, 675.

BTD-^{b}CO$_2$^{t}Bu. ^1H NMR (300 MHz, $CDCl_3$, δ_{ppm}): 7.91 (br, s, 2H), 7.19 (s, 2H), 6.51 (s, 2H), 4.59 (s, 4H), 2.12 (br, m, 12H), 1.94 (br, s, 12H), 1.39 (br, s, 54H). GPC (THF, polystyrene standard): $M_w = 16\,250$, $M_n = 11\,690$, PDI = 1.40. FT-IR (ν_{max}, KBr pellet): 3405, 2978, 2936, 2679, 2494, 2204, 1731, 1693, 1519, 1486, 1457, 1393, 1368, 1312, 1281, 1256, 1213, 1154, 1101, 1056, 954, 847, 758, 721.

BTD-^{b}CO$_2$Na. ^1H NMR (300 MHz, D_2O/DMSO-d_6 (v/v, 1/1), δ_{ppm}): 7.88 (br, s, 2H), 7.22 (br, s, 2H), 4.83 (s, 4H). FT-IR (ν_{max}, KBr pellet): 3391, 2951, 2204, 1667, 1566, 1403, 1283, 1207, 1097, 1061, 838, 778, 721, 667.

TBT-^{b}CO$_2$^{t}Bu. ^1H NMR (500 MHz, $CDCl_3$, δ_{ppm}): 8.10 (s, 2H), 7.95 (s, 2H), 7.52 (s, 2H), 7.10 (s, 2H), 6.45 (s, 2H), 4.55 (s, 4H), 2.24 (m, 12H), 2.08 (m, 12H), 1.38 (s, 54H). ^{13}C NMR (125 MHz, $CDCl_3$, δ_{ppm}): 172.4, 166.6, 152.4, 152.2, 141.8, 134.1, 128.0, 126.0, 124.0, 117.4, 114.2, 90.5, 80.8, 68.5, 58.0, 29.8, 28.3. GPC (THF, polystyrene standard): $M_w = 37\,817$, $M_n = 16\,771$, PDI = 2.26.

TBT-^{b}CO$_2$Na. ^1H NMR (300 MHz, D_2O/DMSO-d_6 (v/v, 1/1), δ_{ppm}): 8.20 (br, 4H), 7.55 (br, 2H), 7.40 (br, 2H), 7.18 (br, 2H), 4.62 (br, 4H), 2.20 (br, 12H), 1.90 (br, 12H).

Hydrolysis of Polymers with Cationic Side Chains. The organic precursor polymer was dissolved in 20 mL of dioxane. The polymer solution was then cooled to 0−5 °C using an ice/water bath. Concentrated HCl (7 mL, 4 N) was added dropwise to the stirred solution. Upon completion of the addition the reaction mixture was warmed to room temperature and stirred for another 12 h. The polymer was then precipitated by pouring the solution into a large amount of acetone (200 mL). The precipitate was collected, washed with acetone (100 mL), and finally dried under vacuum (yield: 90−100%). No further purification was done on these polymers, and they were stored as solid powders in a desiccator and can be redissolved in water easily.

Ph-^{b}NH^{t}Boc. ^1H NMR (500 MHz, $CDCl_3$, δ_{ppm}): 7.61 (br, s, 4H), 7.05 (s, 2H), 6.62 (br, 2H), 4.92 (s, 6H), 4.48 (s, 4H), 3.09 (br, 12H), 1.93 (br, 6H), 1.79 (br, 6H), 1.39 (s, 54H). ^{13}C NMR (125 MHz, $CDCl_3$, δ_{ppm}): 156.6, 132.2, 80.0, 57.0, 46.8, 36.0, 35.8, 28.2. GPC (THF, polystyrene standard): $M_w = 105\,640$, $M_n = 24\,080$, PDI = 4. 40). FT-IR (ν_{max}, KBr pellet): 3393, 2977, 1691, 1517, 1457, 1392, 1367, 1274, 1252, 1170, 1046, 866, 839, 781, 637, 601.

Ph-^{b}NH$_3$Cl. ^1H NMR (300 MHz, D_2O/DMSO-d_6 (v/v, 1/1), δ_{ppm}): 7.61 (br, s, 4H), 7.18 (s, 2H), 4.66 (s, 4H), 2.92 (br, s, 12H), 2.05 (br, 2, 12H). FT-IR (ν_{max}, KBr pellet): 3392, 3031, 2202, 2002, 1672, 1607, 1516, 1489, 1407, 1281, 1191, 1063, 1017, 966, 906, 842, 786, 721, 548.

BTD-^{b}NH^{t}Boc. ^1H NMR (300 MHz, $CDCl_3$, δ_{ppm}): 7.94 (br, s, 2H), 7.25 (br, s, 2H), 4.97 (s, 6H), 4.58 (s, 4H), 3.09 (s, 12H), 1.94 (s, 12H), 1.40 (s, 54H). ^{13}C NMR (125 MHz, $CDCl_3$, δ_{ppm}): 156.5, 132.0, 128.5, 79.8, 57.0, 46.5, 36.0, 35.8, 28.2, 9.5. GPC (THF, polystyrene standard): $M_w = 44\,700$, $M_n = 12\,320$, PDI = 3.60. FT-IR (ν_{max}, KBr pellet): 3350, 2977, 2939, 2679, 2490, 2203, 1693, 1570, 1458, 1392, 1366, 1279, 1252, 1171, 1041, 966, 892, 866, 780, 634, 564.

BTD-^{b}NH$_3$Cl. ^1H NMR (300 MHz, D_2O/DMSO-d_6 (v/v, 1/1), δ_{ppm}): 8.01 (br, s, 2H), 7.36 (s, 2H), 4.78 (s, 4H), 2.94 (s, 12H), 2.07 (s, 12H). FT-IR (ν_{max}, KBr pellet): 3394, 3035, 2202, 2011, 1672, 1610, 1542, 1509, 1409, 1342, 1281, 1191, 1067, 1020, 965, 893, 852, 786, 632, 563, 509.

■ ASSOCIATED CONTENT

Supporting Information. Experimental description of the synthesis of monomers, NMR spectra following deprotection of ester groups from Ph-$^bCO_2^-$, photographs of polymer solutions under visible and near-UV illumination, solvent-dependent absorption spectra of Ph-$^bNH_3^+$ and BTD-$^bNH_3^+$, fluorescence of ester protected polymers in THF solution, fluorescence excitation spectra, pH-dependent absorption and fluorescence spectra of Ph-$^bNH_3^+$ and BTD-$^bNH_3^+$, and fluorescence decay data for Ph-$^bNH_3^+$ and BTD-$^bNH_3^+$. This material is available free of charge via the Internet at http://pubs.acs.org.

■ AUTHOR INFORMATION

Corresponding Author

*Tel: 352-392-9133. Fax: 352-392-2395. E-mail: kschanze@chem.ufl.edu.

■ ACKNOWLEDGMENT

We thank the United States Department of Energy (Grant DE-FG02-03ER15484) for support of this work.

■ REFERENCES

(1) Thomas, S. W.; Joly, G. D.; Swager, T. M. *Chem. Rev.* **2007**, *107*, 1339.
(2) Jiang, H.; Taranekar, P.; Reynolds, J. R.; Schanze, K. S. *Angew. Chem., Int. Ed.* **2009**, *48*, 4300.
(3) Liu, Y.; Ogawa, K.; Schanze, K. S. *J. Photochem. Photobiol., C* **2009**, *10*, 173.
(4) Durate, A.; Pu, K.-Y.; Liu, B.; Bazan, G. C. *Chem. Mater.* **2011**, *23*, 501.
(5) Chen, L. H.; McBranch, D. W.; Wang, H. L.; Helgeson, R.; Wudl, F.; Whitten, D. G. *Proc. Natl. Acad. Sci. U.S.A.* **1999**, *96*, 12287.
(6) Zhou, Q.; Swager, T. M. *J. Am. Chem. Soc.* **1995**, *117*, 12593.
(7) Liu, B.; Bazan, G. C. *Chem. Mater.* **2004**, *16*, 4467.
(8) Feng, F.; He, F.; An, L.; Wang, S.; Li, Y.; Zhu, D. *Adv. Mater.* **2008**, *20*, 2959.
(9) Ortony, J.; Yang, R.; Brzezinski, J.; Edman, L.; Nguyen, T. Q.; Bazan, G. *Adv. Mater.* **2008**, *20*, 298.
(10) Woo, H.; Vak, D.; Korystov, D.; Mikhailovsky, A.; Bazan, G.; Kim, D. Y. *Adv. Funct. Mater.* **2007**, *17*, 290.
(11) Wang, D. L.; Wang, J.; Moses, D.; Bazan, G. C.; Heeger, A. J. *Langmuir* **2001**, *17*, 1262.
(12) Tan, C.; Pinto, M. R.; Schanze, K. S. *Chem. Commun.* **2002**, 446.
(13) Tan, C.; Atas, E.; Müller, J. G.; Pinto, M. R.; Kleiman, V. D.; Schanze, K. S. *J. Am. Chem. Soc.* **2004**, *126*, 13685.
(14) An, L.; Wang, S.; Zhu, D. *Chem.—Asian J.* **2008**, *3*, 1601.
(15) Garcia, A.; Nguyen, T.-Q. *J. Phys. Chem. C* **2008**, *112*, 7054.
(16) Kim, I.-B.; Bunz, U. H. F. *J. Am. Chem. Soc.* **2006**, *128*, 2818.
(17) Wang, F.; Bazan, G. C. *J. Am. Chem. Soc.* **2006**, *128*, 15786.
(18) Swager, T. M. *Acc. Chem. Res.* **2008**, *41*, 1181.
(19) Huang, Y.-Q.; Fan, Q.-L.; Lu, X.-M.; Fang, C.; Liu, S.-J.; Yu-Wen, L.-H.; Wang, L.-H.; Huang, W. *J. Polym. Sci., Part A: Polym. Chem.* **2006**, *44*, 5778.
(20) Jiang, D.-L.; Choi, C.-K.; Honda, K.; Li, W.-S.; Yuzawa, T.; Aida, T. *J. Am. Chem. Soc.* **2004**, *126*, 12084.
(21) Zhu, B.; Han, Y.; Sun, M.; Bo, Z. *Macromolecules* **2007**, *40*, 4494.
(22) Xu, Q.; An, L.; Yu, M.; Wang, S. *Macromol. Rapid Commun.* **2008**, *29*, 390.
(23) Wu, M.; Kaur, P.; Yue, H.; Clemmens, A. M.; Waldeck, D. H.; Xue, C.; Liu, H. *J. Phys. Chem. B* **2008**, *112*, 3300.
(24) Haskins-Glusac, K.; Pinto, M. R.; Tan, C.; Schanze, K. S. *J. Am. Chem. Soc.* **2004**, *126*, 14964.
(25) Jiang, H.; Zhao, X.; Schanze, K. S. *Langmuir* **2006**, *22*, 5541.
(26) Kim, I.-B.; Phillips, R.; Bunz, U. H. F. *Macromolecules* **2007**, *40*, 5290.
(27) Zhao, X. Y.; Schanze, K. S. *Chem. Commun.* **2010**, *46*, 6075.
(28) Wu, Y.-Q.; Limburg, D. C.; Wilkinson, D. E.; Vaal, M. J.; Hamilton, G. S. *Tetrahedron Lett.* **2000**, *41*, 2847.
(29) Zhao, X.; Pinto, M. R.; Hardison, L. M.; Mwaura, J.; Müller, J.; Jiang, H.; Witker, D.; Kleiman, V. D.; Reynolds, J. R.; Schanze, K. S. *Macromolecules* **2006**, *39*, 6355.
(30) Jiang, H.; Zhao, X.; Schanze, K. S. *Langmuir* **2007**, *23*, 9481.
(31) Hardison, L. M.; Zhao, X.; Jiang, H.; Schanze, K. S.; Kleiman, V. D. *J. Phys. Chem. C* **2008**, *112*, 16140.
(32) Pschirer, N. G.; Bunz, U. H. F. *Macromolecules* **2000**, *33*, 3961.
(33) The stock solutions used in this experiment were stored at 0 °C, and they were warmed to room temperature 1 h prior to use. Storing stock solution at room temperature led to slight polymer aggregation in both methanol and water solutions. The aggregation was detected by the appearance of an emission wavelength dependence in the fluorescence excitation spectrum. Note that a distinct red-shifted excimer like band was not observed in the fluorescence spectra. This slight aggregation caused by storage of the stock solutions at ambient can be eliminated by addition of a small aliquot of NaOH (or HCl) solution to adjust the pH of the medium.
(34) Levitus, M.; Schmieder, K.; Ricks, H.; Shimizu, K. D.; Bunz, U. H. F.; Garcia-Garibay, M. A. *J. Am. Chem. Soc.* **2001**, *123*, 4259.
(35) Bunz, U. H. F. *Chem. Rev.* **2000**, *100*, 1605.
(36) Kato, S.-i.; Matsumoto, T.; Ishi-i, T.; Thiemann, T.; Shigeiwa, M.; Gorohmaru, H.; Maeda, S.; Yamashita, Y.; Mataka, S. *Chem. Commun.* **2004**, 2342.
(37) Wong, W.-Y.; Wang, X.-Z.; He, Z.; Djurisic, A. B.; Yip, C.-T.; Cheung, K.-Y.; Wang, H.; Mak, C. S. K.; Chan, W.-K. *Nature Mater.* **2007**, *6*, 521.
(38) Pinto, M. R.; Kristal, B. M.; Schanze, K. S. *Langmuir* **2003**, *19*, 6523.
(39) Zhang, L.; Nguyen, T. L. U.; Bernard, J.; Davis, T. P.; Barner-Kowollik, C.; Stenzel, M. H. *Biomacromolecules* **2007**, *8*, 2890.
(40) Friedman, A. E.; Chambron, J. C.; Sauvage, J. P.; Turro, N. J.; Barton, J. K. *J. Am. Chem. Soc.* **1990**, *112*, 4960.
(41) Fakis, M.; Anestopoulos, D.; Giannetas, V.; Persephonis, P. *J. Phys. Chem. B* **2006**, *110*, 24897.
(42) Jones, G.; Jackson, W. R.; Choi, C. Y.; Bergmark, W. R. *J. Phys. Chem.* **1985**, *89*, 294.
(43) Harriman, A. *Chem. Commun* **1977**, 777.
(44) Thornton, N. B. Ph.D. Dissertation, University of Florida, 1995.